

Dynamic behavior and liquefaction assessment of silver-gold tailings using cyclic direct simple shear (Cyclic DSS) tests and 1d nonlinear site response analysis.

Carlos Omar Vargas-Moreno, Jorge Guillén-Guillén and Ruben Reyes-Hernández.
WSP México, México, omar.vargas2@wsp.com

ABSTRACT: This article presents the estimation of the dynamic behavior and liquefaction assessment in silver-gold tailings using Cyclic Direct Simple Shear (Cyclic DSS) tests. The testing program is presented according to site and design conditions, including the definition of the number of equivalent cycles (N), cyclic stress ratio (CSR), and confining stresses. Additionally, considerations for sample reconstitution using the wet tamping method are presented. Results are presented in terms of stress paths, cyclic resistance curves, and measurements of excess pore pressure ratio, as well as the estimation of post-cyclic monotonic loading. These results were used to evaluate the liquefaction phenomenon under site-specific conditions and for an upstream tailings dam section. Furthermore, based on laboratory results, one-dimensional nonlinear site response models were developed using excess pore pressure generation models. The experimental results were compared with those published in the literature for other tailings and soils, while the site response analysis results were compared with empirical methods.

KEYWORDS: Cyclic direct simple shear, site-response, liquefaction, dynamic behavior, excess pore pressure

1 INTRODUCTION

The characterization and dynamic response of tailings are fundamental for assessing the stability of Tailings Storage Facilities (TSFs). In facilities where liquefaction is a potential hazard, its evaluation becomes particularly critical, since the onset of liquefaction during seismic loading is strongly dependent on site-specific seismic conditions. Dynamic characterization, commonly employed in numerical modeling, requires advanced laboratory testing methods to adequately capture liquefaction phenomena. Among the available techniques, the Cyclic Direct Simple Shear (Cyclic DSS) test provides the most representative conditions for simulating cyclic loading. An additional key consideration is the determination of residual or post-cyclic shear strength, which often deviates substantially from values predicted by empirical correlations, particularly in the context of dynamic soil behavior.

Laboratory-based liquefaction assessment offers a robust framework for investigating this phenomenon. The cyclic direct simple shear test is capable of reproducing the common stress conditions associated with vertically propagating shear waves much more accurately than the cyclic triaxial test. It is therefore particularly useful for liquefaction, cyclic softening, and seismic compression evaluations (Kramer and Stewart, 2025).

Moreover, the use of dynamic test results enables a more accurate evaluation of liquefaction potential, either through nonlinear site response analyses (time domain) with pore pressure generation models or by means of numerical simulations employing advanced constitutive models. The site response analysis approach is particularly relevant, as it allows the simulation of seismic wave propagation and the quantification of the excess pore pressure ratio (r_u), calibrated and supported by cyclic laboratory tests. This integration establishes a more rigorous and consistent framework for evaluating liquefaction susceptibility.

The dynamic behavior of tailings is fundamental for the design and evaluation of the seismic performance of tailings dams, where liquefaction susceptibility is a dominant factor in the stability of these structures, particularly those constructed using the upstream method. One of the principal challenges lies in the dynamic characterization of tailings, in which the dynamic behavior of tailings is strongly influenced by their microstructural fabric and the mineralogical composition of the extracted ore. Previous studies, such as Hu et al. (2017), which investigated the mineralogical behavior of iron and copper tailings, demonstrated notable differences in cyclic

performance, especially in fine-grained materials. Research on fine-grained mine tailings has consistently shown their high susceptibility to liquefaction under cyclic loading. Early studies (Vick 1983; Moriwaki et al. 1982; Ishihara et al. 1980, 1981) reported contractive behavior and reduced cyclic resistance, while later work (McKee et al. 1979; Poulos et al. 1985; Peters & Verdugo 2003) confirmed that increasing fines content decreases shear resistance at constant void ratios. Wijewickreme and Sanin (2005) demonstrated, through constant-volume cyclic direct simple shear (DSS) testing, that fine-grained tailings exhibit progressive stiffness degradation, pore-pressure accumulation, and cyclic mobility comparable to the behavior of natural silts and dense sands. Collectively, these findings highlight the limitations of empirical liquefaction criteria and the need for advanced laboratory testing.

This study focuses on the estimation of dynamic behavior and the evaluation of liquefaction potential in silver-gold tailings through Cyclic Direct Simple Shear (DSS) testing. The experimental program was designed to reflect site-specific and design conditions, including the determination of the number of equivalent loading cycles (N). The characterization of tailings behavior is defined both in terms of laboratory test results and through comparison with published data for other types of tailings and soils. Furthermore, the application of these results in nonlinear site response analyses with pore pressure generation models is presented, providing a practical benchmark against outcomes derived from conventional empirical methods.

2 SITE CONDITIONS AND TESTING PROGRAM

2.1 Site conditions

The work focuses on a tailings dam constructed using the upstream method and founded on competent bedrock, with stored tailings corresponding to conventional or slurry tailings. The initial stage consists of a starter rockfill dam with a height of 15 meters, followed by upstream raises reaching approximately 40 meters. The geotechnical characterization of the foundation indicates competent bedrock with shear wave velocities exceeding 750 m/s. Figure 1 presents a schematic cross-section of the tailings dam, highlighting the piezometric conditions within the conventional tailings, as well as the location of piezocone tests and standard penetration tests used to obtain disturbed samples for the reconstitution of specimens in the laboratory. The tailings are derived from silver and gold extraction, originating from high-grade epithermal vein deposits rich in precious metals. The slurry tailings exhibit the

following geotechnical characteristics: USCS classification as low-plasticity silt, loose density, average shear wave velocities ranging from 150 to 200 m/s, and a specific gravity of solids of approximately 2.2, which values are consistent with those reported by Blight and Steffen (1979) for gold-silver tailings.

Based on the results of the four Seismic Piezocone Penetration Tests (SCPTu) shown in Figure 1, the tailings are generally classified as silty sand, sandy silt, and sand according to the Soil Behavior Type (SBT) chart using normalized CPT parameters. In addition, profiles P1 and P3 exhibit behavior associated with sand-like soils, where cyclic liquefaction is possible depending on the level and duration of cyclic loading. Conversely, profiles P4 and P2 display behavior consistent with clay-like soils, corresponding to cyclic softening and potential flow-liquefaction strength loss depending on soil sensitivity and plasticity, loading conditions, and ground geometry. Figure 2 shows the SCPTu results obtained from the P4 profile, which illustrate the evaluation of the liquefaction susceptibility of the tailings. Additionally, these tailings correspond to hard rock tailings, classified as sandy silt with none to low plasticity, according to the ICOLD geotechnical classification (2025) (see

Figure 3). Based on the geometric conditions and construction type of the tailings dam, as well as its geotechnical and piezometric characteristics, it can be inferred that the tailings dam is susceptible to liquefaction. However, to assess its vulnerability under seismic conditions, it is necessary to determine whether the site's seismic demand is sufficient to trigger liquefaction.

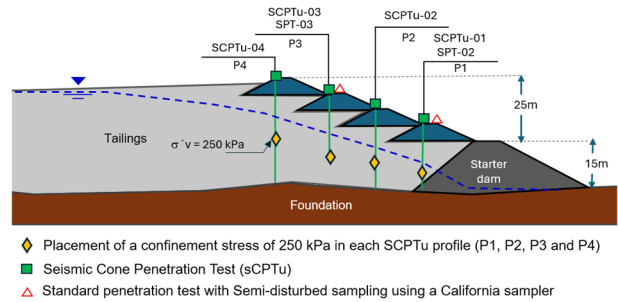


Figure 1. Hypothetical cross-section of the tailings dam.

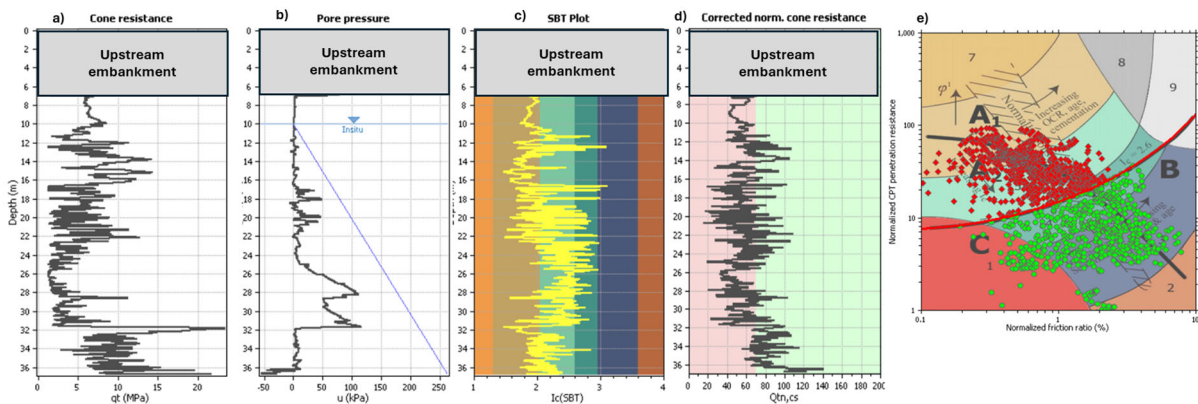


Figure 2. SCPTu-04 (Profile P4). Results of SCPTu: a) Cone resistance versus depth, b) pore pressure versus depth, c) Soil behavior type index versus depth, d) normalized clean sand equivalent cone versus depth and e) Qtn-Fr chart.

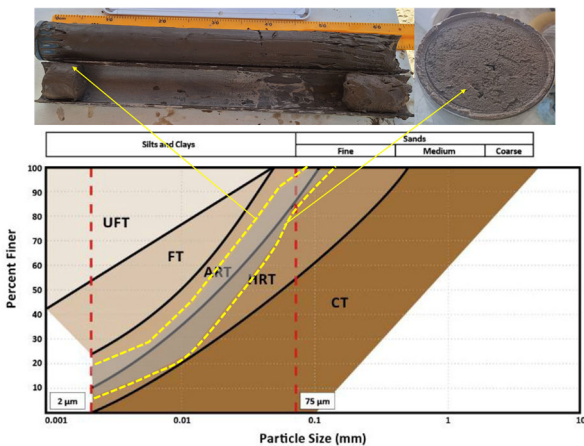


Figure 3. Grain size distribution of Gold-Silver tailings according to the indicative gradation ranges for tailings classification types by ICOLD, 2025.

2.2 Site Seismicity

The site conditions for laboratory testing and liquefaction potential evaluation were considered to correspond to a location within a zone of moderate seismicity, as defined by the seismic region map of the Mexican Republic (CFE, 2017). Based on seismic hazard studies, parameters were estimated to include a peak ground acceleration (PGA) of 0.15 g and a Seismic magnitude (Mw) of 7.0, associated with a return period of

10,000 years. These parameters were employed to calculate the cyclic stress ratio (CSR) using simplified methods (Seed and Idriss, 1971). Cyclic stress ratio (CSR) values on the order of 0.1 were estimated; therefore, this value was selected as the initial reference, and an additional test point was decided at a CSR value of 0.2.

2.3 Laboratory testing program

Two consolidated undrained cyclic direct simple shear (CDSS) tests were conducted, and the specimens were reconstituted using the wet tamping method. The initial test conditions and corresponding specifications are presented in Table 1.

Figure 3 presents images of disturbed tailings samples obtained with a California sampler tube, which were employed for the reconstitution of test specimens. These samples were utilized to produce a material blend (composite material) and to serve as the basis for specimen preparation. Sample reconstitution was performed using the moist tamping method, with the primary objective of achieving a target compaction of $\gamma_d = 14 \text{ kN/m}^3$ at a moisture content between 20% and 25%. This condition was selected to simulate a loose material state, representative of the in-situ conditions of the study area.

This study presents the results of two Consolidated Undrained Cyclic Direct Simple Shear (CDSS) tests performed on tailings, programmed under a confining stress of 250 kPa and cyclic stress ratios (CSR) of 0.1 and 0.2. The CSR values were defined using empirical methods, based on the generation

of one-dimensional soil profiles and the selection of the expected CSR range. An equivalent number of cycles (N_{eq}) equal to 10 was estimated from the average curve proposed by Seed et al. (1975a), considering a seismic magnitude of 7.00. However, the tests were cycled until a simple shear strain of 5% was reached, in order to ensure compliance with the liquefaction failure criterion. In CDSS tests, a 3.75% shear strain (single-amplitude) is often used as a threshold, when a sample reaches this strain level, it's considered to have reached a critical state where the soil is on the verge of liquefaction (Soysa and Wijewickreme, 2014). Liquefaction was defined as 3.75% single amplitude shear strain, which is one of the common liquefaction triggering criteria (NRC 1985, Ishihara 1993, Porcino et al. 2009). Furthermore, similar threshold values have been identified in low-plasticity fine-grained soils (Wijewickreme et al., 2005).

Table 1. Initial and final testing conditions and experimental considerations

	Test Specimen 1	Test Specimen 2
Visual description:	Moist, brown silty clay with sand	
Initial moisture content, %	20.8	20.8
Final moisture content, %	18.7	19.2
Fines content, %	80%	85%
Initial dry density, kN/m ³	13.99	13.99
Initial void ratio	0.89	0.94
Void ratio after consolidation	0.76	0.75
Vertical consolidation stress, kPa	250	250
Initial horizontal stress, kPa	250	250
Cyclic stress ratio	0.1	0.2
Frequency, Hz	0.1	0.1
Nominal rate of shear strain, %/hr	5	5
Test Equipment. Top and bottom box (circular) = 6.35 cm diameter. Load cells and LVDT's connected to data acquisition system for shear force, normal load, horizontal and vertical displacement; surface area = 31.67 cm ² , soil height = 2.54 cm. Stacked Ring set-up used, which included porous stones with pins. Note: Target Compaction 14 kN/m ³		

3 BEHAVIOR UNDER CYCLIC LOADING

3.1 Stress paths and pore pressures under cyclic loading

Figure 4 presents the results in terms of stress path, pore water pressure, and stress-strain paths obtained from the test conducted under a cyclic stress ratio of 0.1 and a confining stress (σ'_c) of 250 kPa. As shown in Figure 4(b), a constant shear strain was maintained during the first 50 cycles; thereafter, the deformation trajectory progressively lost symmetry with respect to the cycles, indicating an approach toward failure conditions. This behavior was accompanied by a gradual accumulation of pore water pressure in each cycle (Figure 4c), reaching excess pore pressure ratio (r_u) values of approximately 0.8 at 50 cycles. Although the theoretical threshold for liquefaction is $r_u = 1.0$, values near 0.8 are commonly considered indicative of liquefaction in these materials.

In terms of stress path (Figure 4d), it was observed that during the first quarter of the loading cycle, the effective stress path shifted leftward, exhibiting a contractive response similar to that expected under monotonic loading, which resulted in an increase in pore pressure. During the reverse shear phase, however, the path descended with an almost vertical slope

($d\sigma'_v/d\tau$), indicating a limited contractive response of the material (Kramer and Stewart, 2025). This behavior was accompanied by a slower rate of pore pressure generation than would typically be expected in a highly contractive material subjected to the same level of cyclic loading (Figure 4d). As the load reversed, shear strain decreased, while pore pressure continued to rise, causing the stress path to progressively shift further to the left.

The stress paths revealed a progressive reduction in effective stress as cyclic loading advanced, accompanied by a gradual accumulation of pore pressure. During the first 25 cycles, a relatively high rate of pore pressure generation per cycle was observed, which subsequently decreased by nearly 50% as the system approached the phase transformation line. In this test, although zero effective stress was not attained by the end of the cycles, an excess pore pressure ratio (r_u) of 0.95 was reached, indicating that liquefaction had occurred.

In Figure 4(e), the hysteresis loops are presented, where a rapid degradation of material stiffness is evident, suggesting that the tailings exhibit sand-like behavior. In the final loading cycles, the hysteresis loops adopt a banana-shaped form, indicating a complete loss of material stiffness

For the second test, the specimen was reconstituted under the same conditions and properties as the first one, as summarized in Table 1. The objective of this test was to evaluate the material response under a higher cyclic stress ratio (CSR = 0.2). Figure 5 presents the results in terms of stress path, pore water pressure, and stress-strain curves, obtained under a cyclic stress ratio of 0.2 and a confining stress (σ'_c) of 250 kPa.

In Figure 5a, the failure criterion was reached after only five cycles as a consequence of the increased cyclic loading. The shear strain response exhibited a loss of symmetry beginning at the fourth cycle, and the specimen attained the deformation associated with the failure criterion (Figure 5b). In Figure 5c, a constant and rapid rate of pore pressure generation was observed, on the order of 0.2 per cycle. By the end of the test, the excess pore pressure ratio (r_u) reached a maximum value of 0.8; although the theoretical threshold of 1.0 was not attained, the observed stiffness degradation and shear strain provided evidence that liquefaction had occurred.

Regarding the stress path (Figure 5d), predominantly contractive behavior was observed during the first quarter of the loading cycle. Subsequently, the slopes of the reverse paths also exhibited a contractive response, with the trajectory shifting rapidly leftward and producing an accelerated reduction in effective stress, accompanied by a significant loss of stiffness beginning at the third cycle. This behavior was manifested in large deformations during the final hysteresis cycles (Figure 5e), where the cyclic hysteresis loops at high strain levels provided confirmation of the material liquefaction.

Based on the behavior observed in both tests, it was inferred that the reconstitution conditions were very similar for both specimens, as the material exhibited consistency in its cyclic resistance and in the number of cycles attained in each test. The failure criterion of 3.75% shear strain was attained after 53 cycles in the first test (CSR = 0.1) and after only four cycles in the second test (CSR = 0.2). Furthermore, although the materials were classified as low-plasticity sandy silts, the degree of stiffness degradation observed in both specimens confirmed that their cyclic response tends toward sand-like behavior. This tendency was expected, given that the fine particles in these materials, despite their small size, form a relatively strong structure due to their origin from rock grinding and the mineral composition involved.

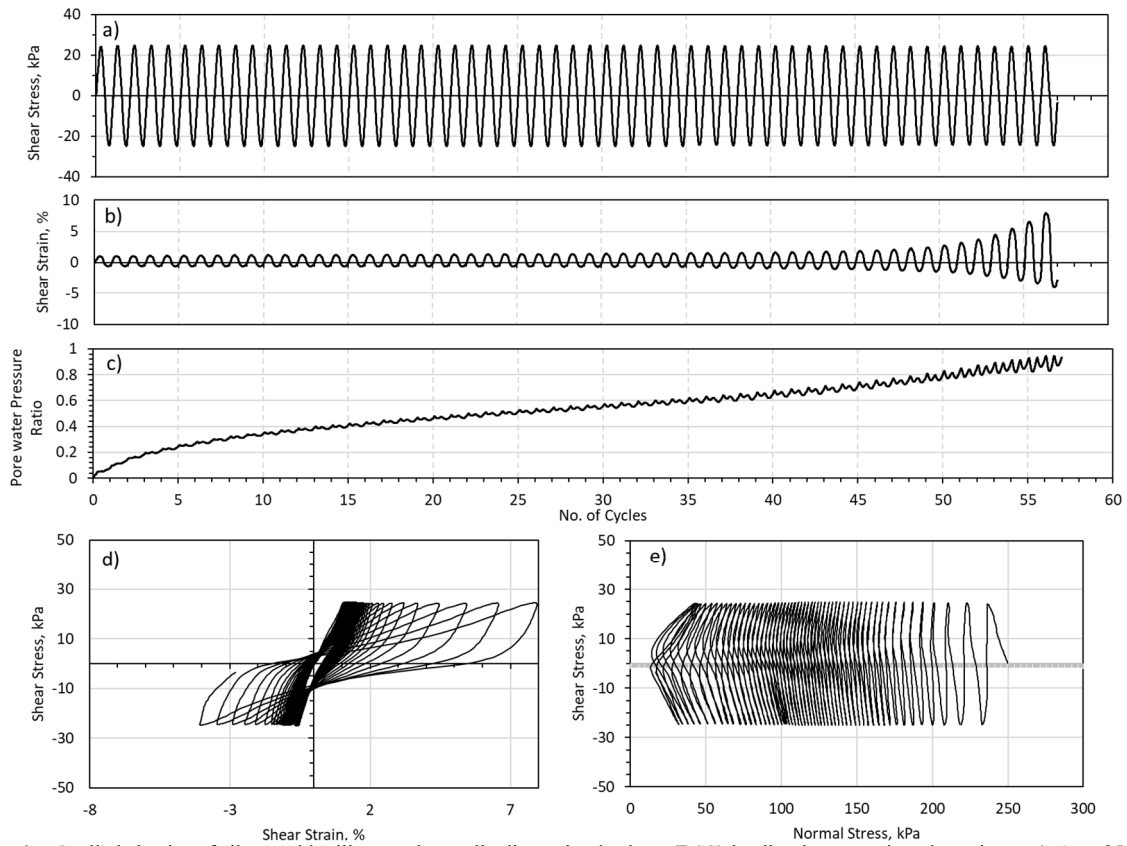


Figure 4. Cyclic behavior of silver-gold tailings under cyclic direct simple shear (DSS) loading in reconstituted specimens ($\sigma'_{vc} = 250$ kPa, CSR = 0.1). a) Shear stress versus number of cycles (N), b) shear strain versus N, c) Pore water pressure ratio versus N, d) cyclic hysteresis loops and e) stress path.

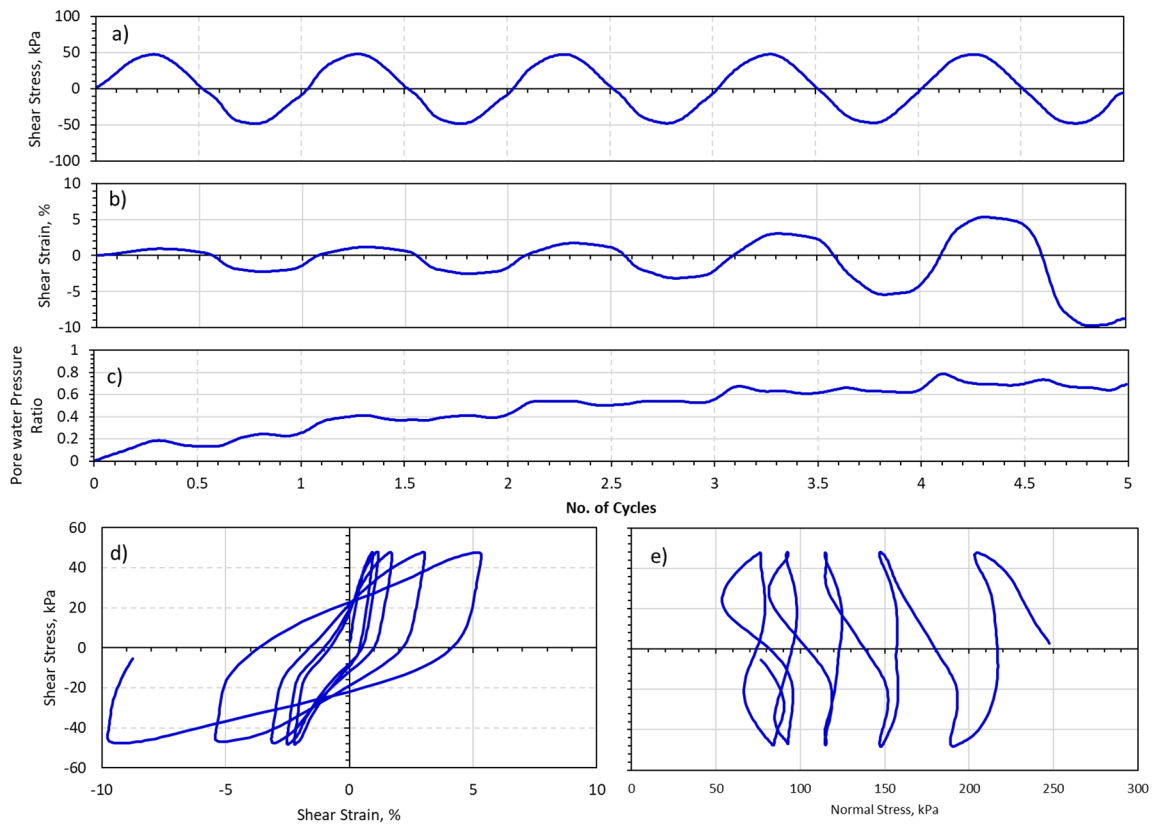


Figure 5. Cyclic behavior of silver-gold tailings under cyclic direct simple shear (DSS) loading in reconstituted specimens ($\sigma'_{vc} = 250$ kPa, CSR = 0.2). a) Shear stress versus number of cycles (N), b) shear strain versus N, c) Pore water pressure ratio versus N, d) cyclic hysteresis loops and e) stress path.

3.2 Cyclic Strength

Based on the results of these tests, the cyclic resistance points at failure (3.75%) were plotted in order to generate the cyclic resistance curve for these materials and compare them with similar ones (Figure 6). In this figure, it can be observed that the silver-gold tailings exhibit lower cyclic resistance than loose sands and even lower than the test results found in the literature. This comparison indicates that the specimens were reconstituted to a slurry-like material consistency, which closely resembles the behavior of loose materials (low relative density). This aspect is highly relevant, as tailings with such density levels are expected in that area. This is supported by the fact that the region shows low standard penetration test blow counts and cone tip resistance measurements below 5 MPa.

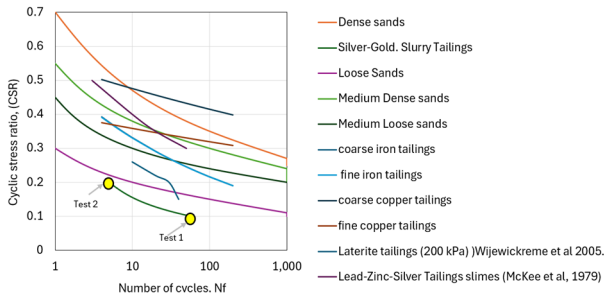


Figure 6. Cyclic stress ratio versus number of cycles to reach γ 3.75% for silver-gold tailings and cyclic resistance curves of various soils and tailings.

3.3 Postcyclic shear strength

For both test specimens, post-cyclic shear tests were conducted to determine the residual strength ratio, which is typically derived from field investigations such as the piezocone (CPTu). Correlations obtained from piezocone data are generally conservative; therefore, these parameters are frequently assigned and applied in the physical stability assessment of tailings storage facilities (TSFs). Although the current criterion for identifying liquefiable materials assumes that liquefaction will occur regardless of the triggering mechanism, representing a conservative yet safe approach that should be adopted under liquefiable conditions, it is important to address in the discussion the extent to which residual strength may be underestimated, particularly in scenarios involving design-level earthquakes or in regions characterized by low seismicity.

Figure 7 (black dashed line) presents the results of post-cyclic test conducted at CSR = 0.1, in which strain hardening was observed during undrained monotonic loading following cyclic loading. The post-cyclic monotonic test conducted after applying cyclic loading at CSR = 0.1 exhibits a progressive increase in shear stress, reaching approximately 50 kPa, while the effective normal stress rises to about 70 kPa. The stress paths for this material indicate strain hardening and a moderately dilative tendency. This suggests that the material retains some strength after cyclic loading but experiences significant strength degradation, a behavior typical of tailings or loose to medium-dense sands under low cyclic stress ratios. The absence of pronounced dilation implies limited recovery of stiffness, confirming that cyclic history strongly influences residual strength and deformation characteristics. Furthermore, the dilative response mobilized up to the ultimate strength is characteristic of cumulative permanent deformations during cyclic loading, which can be associated with cyclic mobility.

Figure 7 (blue solid line) presents the results of the post-cyclic simple shear test for the specimen tested at CSR = 0.2. The stress path for this specimen reveals a pronounced strain-hardening behavior combined with a clear dilative tendency

after an initial contractive phase. The trajectory shows a progressive increase in shear stress up to approximately 50 kPa, while the effective normal stress rises to nearly 90 kPa, indicating substantial recovery of effective stress during monotonic loading. This response suggests that, although the material experienced significant strength degradation due to prior cyclic loading, it retains the ability to mobilize dilation as ultimate strength is approached.

In both tests, the residual strength ratio (S_r/σ'_v) was approximately 0.18. Based on CPTu tests conducted in the same area, these tailings typically exhibit peak undrained strength ratios (S_u/σ'_v) around 0.25, and residual strength ratios (S_r/σ'_v) near 0.05. Considering the relationship between the strength obtained from CPTu tests and the residual strength ratio (S_r/σ'_v) derived from laboratory experiments, it is indicated that cyclic loading reduced the strength by approximately 30% in its ultimate state, whereas the reduction or loss of strength ratio estimated from CPTu data would be about 80%.

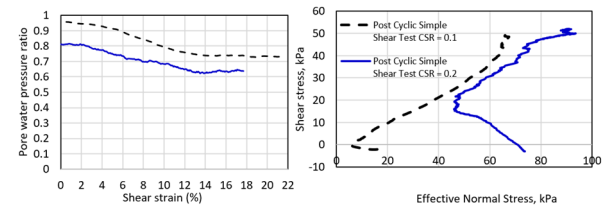


Figure 7. Post cyclic simple shear test results.

3.4 Pore water pressure ratio

In Figure 8, a comparison between pore water pressure ratio (ru) curves for various soils and tailings, including the gold–silver tailings under study, is presented. It is shown that the ru curve for the gold–silver tailings exhibit behavior similar to that observed for fine copper and iron tailings. Based on these results, it can be inferred that fine tailings tend to display behavior characteristic of slimes, as defined by Moriwaki et al. (1982). This similarity provides insight into the cyclic behavior of the studied tailings, consistent with the general trends observed in low-plasticity fine materials. In Table 2, a summary of the main results from the dynamic tests is presented.

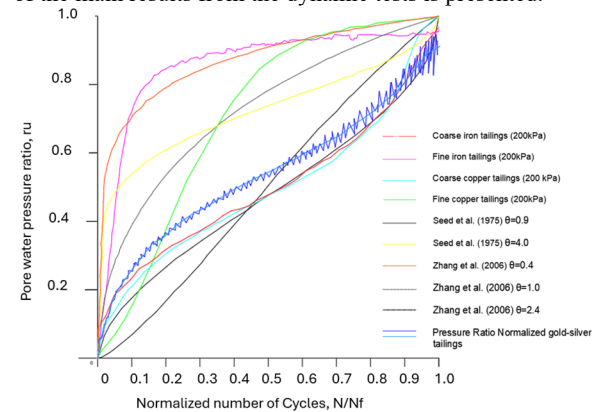


Figure 8. Pore pressure ratio curves for gold tailings and other soils and tailings.

4 LIQUEFACTION ASSESSMENT THROUGH ONE-DIMENSIONAL NONLINEAR SITE RESPONSE ANALYSES

To demonstrate the application of the test results and their impact on the evaluation of seismic liquefaction potential, one-dimensional nonlinear site response analyses (NL-SRA-1D) were performed using excess pore pressure generation models. These analyses were conducted to estimate site response and compare it with empirical or simplified methods. For the

analyses, data from SCPTu-04 (Figure 1) were selected, and a soil profile was generated for both the NL-SRA-1D simulations and the simplified liquefaction assessment. For the case study, the liquefaction potential analyses that were carried out based on the data from profile P4. For the NL-SRA-1D evaluation, the input motion consisted of a synthetic earthquake record generated for the site, as shown in Figure 9, representing the base motion applied at the model foundation. The NL-SRA-1D simulations adopted the GMP model (Green et al., 2000), as it provided the most representative calibration of excess pore pressure generation in the tested samples (Figure 10). Figure 11 presents the liquefaction assessment results obtained using NL-SRA-1D and the results based on CSR estimation through the empirical approach and CRR derived from SCPTu-04 data.

Table 2. Summary of results of CDSS tests.

Parameter	Test	Test
	Specimen 1	Specimen 2
Number of cycles completed	57	5
Number of cycles at failure (3.75%)	54	4
Max. Pore water pressure ratio (r_u)	0.95	0.8
Measured Post-Cyclic Peak Shear Stress, kPa	46.3	48.4
Sr/σ'_{vc}	0.18	0.18

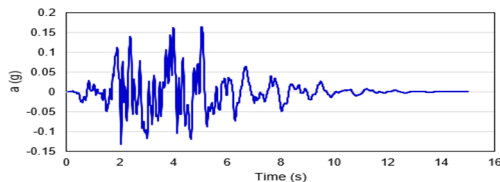


Figure 9. Input motion.

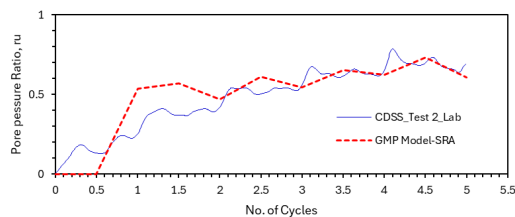


Figure 10. Calibration of the excess pore water pressure model.

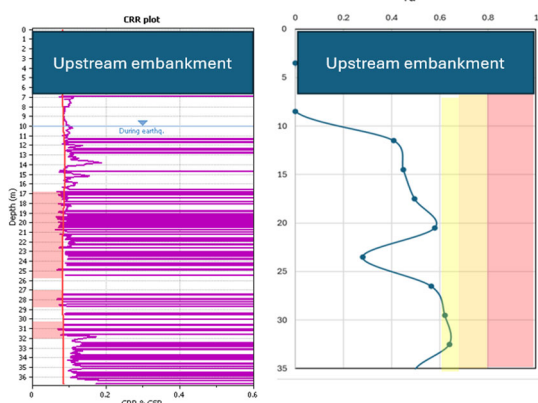


Figure 11. Liquefaction Assessment through Simplified Methods and NL-SRA-1D and

The results of the liquefaction evaluation using pore pressure generation models calibrated with laboratory data (Test 2) indicate that, under the input earthquake conditions ($PGA = 0.15 \text{ g}$), certain zones would reach liquefaction. This behavior is consistent with laboratory observations, as excess pore pressure ratios similar to those obtained in the tests are

observed at the confinement levels present in the soil profile. Furthermore, the CRR–CSR profile also identifies zones susceptible to liquefaction; however, the results remain consistent when compared with those derived from site response analysis (SRA), considering that empirical procedures tend to be more conservative

5 CONCLUSIONS

- Silver–gold tailings exhibit high liquefaction susceptibility due to their low density, low plasticity, and contractive response under cyclic loading, behaving similarly to loose sands, particularly under moderate seismic conditions.
- Cyclic Direct Simple Shear (CDSS) tests effectively characterize this response, revealing significant pore pressure buildup, stiffness degradation, and shear stress evolution. The cyclic stress ratio (CSR) is critical: an increase from 0.10 to 0.20 reduces the number of cycles to failure from 54 to only 4.
- Although classified as low-plasticity silty sands, the tailings display sand-like behavior, with rapid stiffness loss under cyclic loading.
- Post-cyclic shear strength tests indicate residual strength ratios near 0.18, substantially higher than empirical estimates derived from CPTu data, which tend to be conservative.
- Nonlinear site response analysis (NL-SRA-1D) using calibrated pore pressure generation models provides a more reliable liquefaction assessment compared to simplified empirical methods

6 REFERENCES

- Blight, G.E., and Steffen, W.L. (1979). Properties of gold and silver tailings. Proceedings of the Symposium on Tailings Disposal, South African Institute of Mining and Metallurgy.
- CFE (2017). Mapa de regiones sísmicas de la República Mexicana. Comisión Federal de Electricidad.
- Hu, Y., Li, X., and Wang, G. (2017). Mineralogical influence on dynamic behavior of tailings. Journal of Geotechnical and Geoenvironmental Engineering, ASCE.
- ICOLD (2022). Tailings Dam Safety. Bulletin No. 194, Version 1.0, International Commission on Large Dams (ICOLD), Committee L – Tailings Dams and Waste Lagoons.
- Ishihara, K. (1993). Liquefaction and flow failure during earthquakes. Geotechnique, 43(3), 351–415.
- Kramer, S.L., and Stewart, J.P. (2025). Advanced soil behavior under cyclic loading. In preparation for ICOLD guidelines update.
- Marcuson, W.F., and Hynes, M.E. (1990). Evaluation of liquefaction potential using laboratory data. Proceedings of the International Workshop on Recent Advances in Geotechnical Earthquake Engineering and Soil Dynamics.
- Moriwaki, Y., Seed, H.B., and Idriss, I.M. (1982). Behavior of tailings under cyclic loading. Report No. UCB/EERC-82/10, University of California, Berkeley.
- Porcino, D., Diano, A., and Silvestri, F. (2009). Cyclic simple shear tests on natural silty soils. Soil Dynamics and Earthquake Engineering, 29, 1058–1071.
- Seed, H.B., and Idriss, I.M. (1971). Simplified procedure for evaluating soil liquefaction potential. Journal of Soil Mechanics and Foundations Div., ASCE.
- Seed, H.B., Tokimatsu, K., Harder, L.F., and Chung, R.M. (1985). Influence of SPT procedures in soil liquefaction resistance evaluations. Journal of Geotechnical Engineering, ASCE.
- Soysa, H., and Wijewickreme, D. (2014). Cyclic shear response of low-plasticity silt and silty sand. Canadian Geotechnical Journal, 51(6), 686–703.
- Wijewickreme, D., Sanin, M., and Byrne, P.M. (2005). Cyclic shear response of fine-grained soils. Canadian Geotechnical Journal, 42, 126–140.